# FUNDAMENTALS OF THERMOELECTRIC MATERIALS

## Abstract

Thermoelectric materials possess the ability to transform waste heat into electrical energy and works inversely. The dimensionless quantity is used to determine the conversion efficiency is called the figure of merit (ZT). For many researchers, exploring a material with a good ZT value is a big challenge. The ZT value is influenced by key factors such as electrical conductivity, Seebeck coefficient, and thermal conductivity. This chapter discuss about the measuring techniques and strategies towards enhanced electrical conductivity, improved Seebeck coefficient and reduced thermal conductivity and also written about the historical background and principles involving in development of thermoelectric materials. This chapter also explained the properties of various types of thermoelectric materials briefly such as Oxides, Skutterudites, Clathrates, Half-Heusler compounds and Zintl-phase materials.

## Authors

**M. Sharath Kumar**
Department of Physics,
University college of Science,
Osmania University,
Hyderabad, Telangana, 500007, India.

**M. Yellesh Kumar**
Department of Physics,
University college of Science,
Osmania University,
Hyderabad, Telangana, 500007, India.

**K. Venkataramana**
Department of Applied Sciences,
M.V.S.R. Engineering College,
Nadergul, Hyderabad-501510, India.

**M. Radha**
Department of Physics,
JNTU Hyderabad,
Kukatpally, Hyderabad - 500 085,India.

**N. Pavan Kumar**
Department of Sciences and Humanities,
Matrusri Engineering College, Saidabad,
Hyderabad, Telangana, 500059, India.
pa11akash@gmail.com

## I. INTRODUCTION

Now a days, thermal management and energy efficiency is a vital challenge as waste heat is ubiquitous from the advanced technologies and industries. To address these issues, one possible technology i.e. thermoelectric (TE) is to be employed, which can transform the waste heat into electricity. This technology makes use of materials that are referred to as TE materials because of their capacity to generate electrical potential based on the Seebeck effect with a temperature difference between both ends. The name of the device used to generate TE power is called TE generator (TEG). TEGs are quite beneficial, since no hazardous byproducts are created during operation, very small in size, simple structure, run with noiseless and environmentally friendly manner. In addition to having a long operating life, TEG may generate electricity from low-grade heat at low temperatures [1,2] Based on the range of operating temperatures, these materials can be categorized into three types[3].

- low-temperature materials, where around 400 K is the typical operating temperature. In this temperature range, bismuth-based alloys are among the most commonly used materials.
- Materials that operate at an intermediate temperature, or between 600 and 900 K. In this category, lead-based alloys are frequently utilized.
- Materials with high operating temperatures—those with temperatures above 900 K. Typically, materials made up of silicon and germanium belong within this category.

1. **Historical Background:** Through systematic research, Volta discovered the thermoelectric effect,illustrates that the electromotive force originates from temperature variations at the junctions of dissimilar conducting materials. This pivotal work not only settled scientific disputes but also paved the way for comprehending the direct conversion of thermal and electrical energy. Volta's findings heralded the dawn of thermoelectricity, electromagnetism, and electrochemistry, eventually culminating in the invention of the electrical battery. In 1821, Seebeck provided a comprehensive explanation for thermoelectricity[4] .

2. **Thermoelectric Generator(TEG):** Thermoelectric generator(TEG) is a solid semiconductor apparatus designed to transform the temperature gradient across it to the electrical energy [5].A single thermoelectric can only generate a certain amount of output power and TE voltage.A TEG module is constructed by connecting several P-type and N-type semiconductors in electrical series while being thermally connected in parallel[6]. A Thermoelectric device has the capability to transform the heat into electricity via the seebeck effect ,and conversely ,it can achieve the reverse process ,converting electricity into the heat through the peltier effect[7].

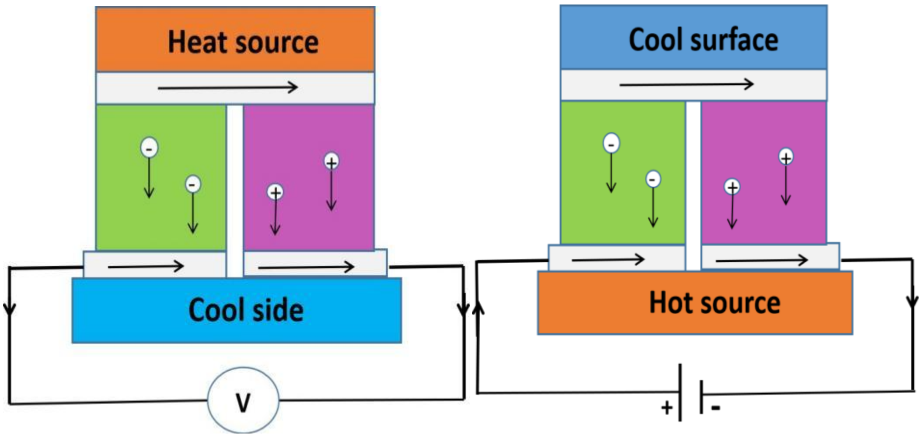

**Figure1:** Mechanism in Seebeck and Peltier effects.

3. **Various advantages of TEG:** Direct energy conversion sets itself apart from numerous heat engines, as it diverges from the usual process where thermal energy is first transformed into mechanical energy and then an alternator is employed to convert that mechanical energy into electricity. The TEG has no moving parts and no operating fluids, thus it requires no maintenance and doesn't cost extra. TEG can generate kilowatts or micro generation in extremely small places. Operation of TEG is noiseless.

## II. PRINCIPLES OF TEM

1. **Seebeck Co-efficient:** The process of transferring heat into the electricity and vice versa is known as thermoelectricity. Another name for this phenomena is Seebeck effect,named after German scientist ,Thomas Seebeck.In 1821Seebeck twisted two wires of different metals and heated one end of them.Thomas Seebeck noticed a tiny amount of current passing through the metal wires .The electrons' movement from one end to other end, which determines the  current flow direction.[8]

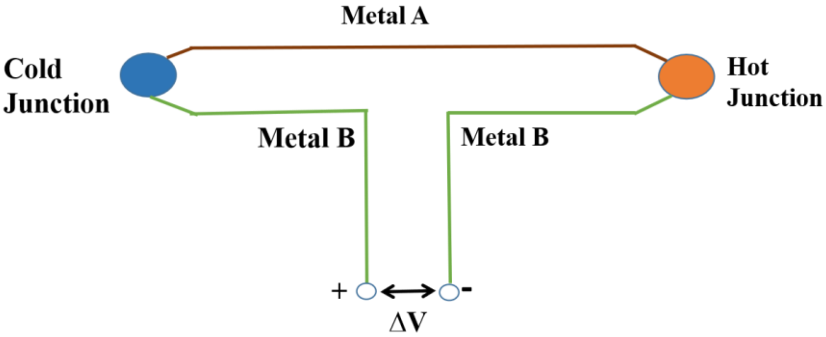

**Figure 2:** Schematic Diagram of Seebeck Effect

Seebeck came to the conclusion heat might produces the electricity.

$$\Delta E \propto \Delta T \qquad (1)$$

where E and T stand for the connections' temperature differences and emf output, respectively.The proportional constant of the Eq(1) is

$S_{ab}= \Delta E \backslash \Delta T$ (2)

Is called Seebeck cofficient .The material's Seebeck coefficient is the characteristic that establishes how well thermocouples work[9].

2. **Peltier Effect:** Seebeck failed to elucidate the true empirical hypothesis underlying this procedure and incorrectly concluded that flowing energy and flowing heat have the same outcome.In 1834 a French scientist discovered ,each side of the twisted wires showed signs of heating and cooling current passed through them[10].

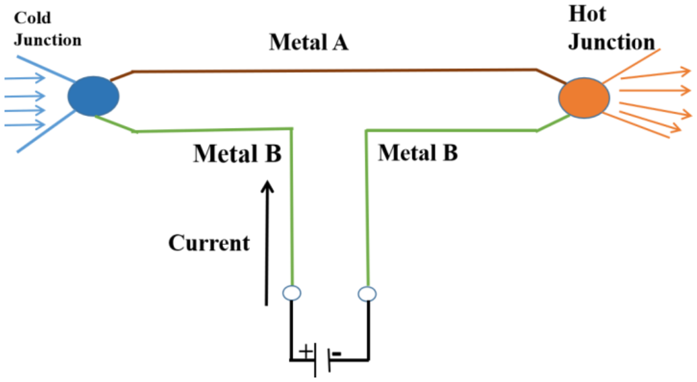

**Figure 3:** Schematic diagram of Peltier effect

It was revealed that
$Q \propto I$ (3)

In this context, Q represents the rate at which heating or cooling occurs.The proportional constant for the above equation is called Peltier coefficient .

$\Pi_{ab} = \frac{Q}{I}$ (4)

In this case $\Pi_{ab} = \Pi_{a}_\Pi_{b}$is the coefficient of the two different metals[11].

3. **Thomson Effect:** In 1854, William Thomson carry out a thorough analysis of the Seebeck and Peltier Effects and explained how they relate to one another. A thermodynamic relationship exists between the Seebeck and Peltier coefficients. William Thomson discovered with a conductor which current folws ,heat can either be absorbed or emitted depending on the material and the direction of current flow when there exists a temperature difference between any two points of the conductor. .This effect is called Thomson effect.

Above three phenomena are called as thermoelectric effects[12].

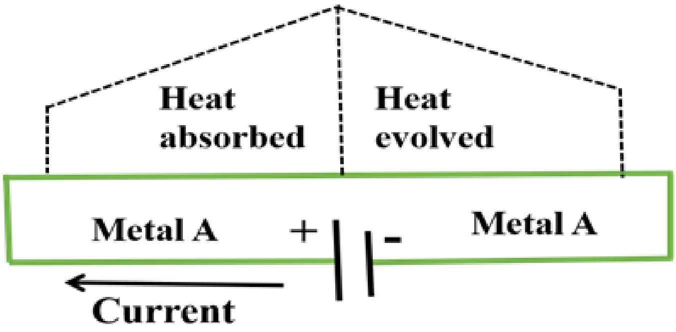

**Figure 4:** Schematic diagram of Thomson effect

The transfer derived by

$$\frac{\delta Q}{\delta x} = rI\frac{dT}{dx} \qquad \text{\_\_\_\_\_\_\_\_\_\_\_\_\_\_\_} (5)$$

$$r = I\frac{\frac{\delta Q}{\delta x}}{\frac{dT}{dx}} \qquad \text{\_\_\_\_\_\_\_\_\_\_\_\_\_\_\_\_} (6)$$

Where r is the Thomson coefficient and $\frac{\delta Q}{\delta x}$is the transfer of thamson heat.

The relation between Seebeck coefficient and Peltier coefficient are derived from first and second law of thermodynamics.

$$\Pi_{ab} = S_{ab}\, T \qquad \text{\_\_\_\_\_\_\_\_\_\_\_\_} (7)$$

$$\frac{r_a - r_b}{T} = \frac{dS_{ab}}{dT} \qquad \text{\_\_\_\_\_\_\_\_\_\_\_\_\_\_\_\_} (8)$$

From the equation (5) and (8) .We get

$$Q = S_{ab} IT \qquad (9)$$

If $S_{ab}$ is high,a big current will be needed to achieve the high Q value[9,13].

## III. POWER FACTOR($S^2\sigma$)

The figure of merit relies on factors like electrical conductivity, Seebeck coefficient, and thermal conductivity. Numerous studies have focused on enhancing the ZT value of thermoelectric materials by methods such as reducing the lattice component of thermal conductivity,This can be accomplished using methods such as introducing rattler atoms into cage-like structures, integrating nanoparticles into the host matrix, or applying nanostructuring to conventional materials. Another approach involves enhancing the power factor by doping impurities [14].

$$\text{Power factor} = S^2\sigma \qquad (10)$$

1. **Seebeck Coefficient:** This is characterized by the ratio of an applied temperature gradient to an electric potential gradient.

$$S = -\left(\frac{\Delta V}{\Delta T}\right) \tag{11}$$

Where $\Delta V$ denotes electric potential and $\Delta T$ is the temperature gradient at specific temperature $T_0$ [15].As per the Pisarenko relationship, the Seebeck coefficient is obtained by dividing the temperature difference by the TE voltage.

$$S_{ab}=Tm^*\frac{8\Pi^2 k_B^2}{3qh^2}\left(\frac{\Pi}{3p}\right)^{2\backslash 3} \tag{12}$$

Where m* denotes the density of states (DOS) effective mass,$k_B$ denotes boltzman constant , h is planks constant,q denotes charge carrier and p denotes the concentration of hole .Modifying the Seebeck coefficient is possible by adjusting both the effective mass and carrier concentration[16] .

- **Measurement of Seebeck coefficient:** Integral method is one of the most well known techniques to measure the Seebeck coefficient. Electric potential can be expressed as

$$V_{ab}(T_1,T_2) =\int_{T_1}^{T_2} S_{ab}(T)\, dT =\int_{T_1}^{T_2}[S_b(T)-S_a(T)]dT \tag{13}$$

In this scenario, $S_a(T)$ represents the absolute Seebeck coefficient of the sample under measurement, whereas $S_b(T)$ signifies the Seebeck coefficient of the reference leads.For the thermoelectric material ,b has Ohmic and isothermal junctions with material a.Both exhibits uniform chemical and physical characteristics. In this method the temperature at one end of the specimen is held constant at $T_1$,while the temperature at other end is adjusted within the range $T_2=T_1+\Delta T$ ,where T represents the temperature variation of interest .A suitable analytical estimate is employed and extended to the whole $V_{ab}(T1,T2)$ dataset, followed by the computation of its derivative with respect to T2.The Eq(13) becomes [17].

$$S_{ab}(T_2) = S_b(T_2) - S_a(T_2) =\frac{dV_{ab}(T_1T_2)}{dT_2} \tag{14}$$

At elevated temperatures, the absolute Seebeck coefficient can be acquired through direct measurement of the Thomson coefficient μ, with subsequent application of Kelvin relation to calculate the Seebeck coefficient i.e.

$$S(T_2) = S(T_1)+\int_{T_1}^{T_2}\frac{\mu}{T}\, dT \quad (T_1<T_2) \tag{15}$$

Here, the base temperature employed to calculate the initial term $S(T_1)$ with the reference of superconductor material( which could be below Tc) and target base temperature are denoted by $T_1$ and $T_2$ [18].

- **Strategies to Improve the Seebeck Coefficient:** Seebeck coefficient can enhance by the one of the technique called quantum confinement .In 1993,Dresselhaus and

Hicks demonstrated that the confinement of electrons or holes in low-dimensional materials enhances thermoelectricity. In the case of low-dimensional materials,the characteristic length of material in specific direction closely aligns with the effective de Brogile wavelength of carrier in the direction. Hence, the movement of carrier is confined in specific direction. Carriers are situated in potential wells enclosed by walls of unbounded height. In this special case, the electronic spectrum undergoes a notable transformation commonly referred to as the quantum size effect[19].

In initial theoretical model, R&D addressed the thermoelectricity within 2D quantum well structures. The assumption made was that the electrons within the valance and conduction band exhibits a straight forward parabolic energy band structure and the electrons are exclusively inhabiting the lowest sub-band within quantum well. The electronic dispersion relation for a two-dimensional system is as follows.

$$\mathcal{E}_{2D}(\mathrm{k_x,k_y}) = \frac{\hbar^2 k_x^2}{2m_x} + \frac{\hbar^2 k_y^2}{2m_y} + \frac{\hbar^2 \Pi^2}{2m_z d_w^2} \qquad (16)$$

The width of the quantum well is denoted by dw,and The effective mass tensor components corresponding to a constant energy surface are denoted as mx, my, and mz..Additionally, it is assumed that current flow takes place along the x-axis, while quantum confinement is present in the z-axis direction . The square 1D quantum wire is characterized by a specific connection

$$\mathcal{E}_{1D}(\mathrm{k_x}) = \frac{\hbar^2 k_x^2}{2m_x} + \frac{\hbar^2 \Pi^2}{2m_y d_w^2} + \frac{\hbar^2 \Pi^2}{2m_z d_w^2} \qquad (17)$$

Where the flow of current takes place in the x- direction, while the y and z directions experienced quantum confinement. The solution for equation were subsquently derived for S, σ and $k_e$ for the 1D and 2D systems[20].

Exploring the Mott equation below provides the valuable insights into the origin of the observed S with improvement in low-dimensional materials

$$S = \frac{\Pi^2 k_B^2 T}{3e}\left[\frac{1}{n}\frac{\partial n(E)}{\partial E} + \frac{1}{\mu}\frac{\partial \mu(E)}{\partial E}\right]_{E=E_f} \qquad (18).$$

Where Boltzmann constant is denoted by $k_B$ ,carrier charge denoted by $e$ and fermi energy denoted by the $E_f$ . If bands exhibits a parabolic relationship between energy and momentum ,formula can be expressed as follows.

$$S = \frac{\Pi^2 k_B^2 T}{3e}\left[\frac{1}{n}\frac{\partial n(E)}{\partial E} + \frac{r-\frac{1}{2}}{E}\right]_{E=E_f} \qquad (19)$$

Where r refers the scattering parameter. From above formula ,improvement of S obtained from the increasing the $r$ and decreasing the $n$ [21].

NguyenT.Hung et al. reported the thermopower values exceeding 2000μV\K at room temparature can be achieved in certain single-walled carbon nanotubes (s-

SWNTs) with diameter smaller than 0.6nm. It is concluded that as single-walled carbon nanotubes(s-SWNTs) diameter decreases, their thermopower increases [22].

2. **Electrical Conductivity($\sigma$):** A material's electrical conductivity (σ) is a measurement of its capacity to carry an electrical current. The carrer mobility (μ) and electrical conductivity $\sigma$ of a semiconductor are related by

$$\sigma = ne\mu \qquad (20)$$

Regarding the charge carrier lattice scattering, it is expected that the temperature is inversely proportional to the free paths length . According to the equation mobility varies with temperature [23].

$$M \propto T^{q/2-1} \qquad (21)$$

3. **Measurement of Electrical Resistivity of TEM:** One of the method for measuring the electrical resistvity is the four-probe bipolar technique, described by

$$\rho = \frac{V}{I}\frac{A}{l_o} \qquad (22)$$

Where averge cross -sectional area denoted by A, effective distance between the centers of the two voltage contacts are denoted by $l_o$, the averaged bipolar voltage is denoted by V, average current through the sample denoted by I.The current passing through the sample can be assessed by measuring the voltage across a high-precision resistor with a predetermined value, which is connected in series with the sample.The selection of the effective distance is based on the condition $l-l_0 \geq 2w$ to guarantee uniform current distribution between the voltage contacts[24]

- **Strategy to Improve Electrical Conductivity :** The challenge of ionized impurity scattering in two-dimensional structures was effectively addressed by deliberately dividing the conduction carriers from their parent atoms in a strategic manner.The method is known by various names, including remote doping,modulation doping or delta doping.Under this scheme,In a semiconductor device,all dopants are concentrated within a narrow doping layer, a region strategically positioned away from the primary transport channel by a spacer. Modulation-doping in the realm of 2D materials has played a crucial role in significantly advancing the semiconductor industry in the past.Optoelectronic devices and efficient transistors have been developed by this technique[25].

- **Electron Filtering:** loffe was introduced the concept of electron filtering(EF) in thermoelectric materials.In 1995 Rowe and Min developed the concept of EF[26]. They explored the effects of different barriers on conductivity (σ) and the Seebeck coefficient (S) using the relaxation-time approximation method. They suggested minority charge carriers movement could be hindered by high-energy barriers, potentially reducing the occurrence of bipolar effects.This clearly demonstrates a reduction in conductivity (σ) through the facilitation of primary charge carrier transport. Nanostructures offer another avenue for boosting the power factor (PF) by employing energy filtering. Nano-sized precipitates serve as filters, selectively allowing charge carriers with higher energy levels to pass through, there by elevating the Seebeck coefficient (S) and consequently enhancing the PF[27].

Quing Tan et al.,synthesized Ag doped SnS through spark plasma sintenring (SPS) and mechanical alloying(MA) method.Incorporating p-type dopants like Ag has proven advantageous in boosting the electrical conductivity (σ) of SnS by augmenting the carrier concentration.They demonstrated a significant increase in σ from 0.001 to 3 $Scm^{-1}$ at 323 K as the Ag doping concentrations increased. At a temperature of 873 K, achieved a promising figure of merit (ZT) value of 0.6 . The results suggest that further improvements in ZT can be attained by optimized doping levels, microstructure, and composition to enhance carrier concentration. Overall, the synthesis of Ag-doped SnS through MA and SPS processes showed it's potential for thermoelectric applications with further optimization[28].

Wenyu Zhao et al., synthesized Ba and In doped with skutterudite compounds $Ba_rIn_sCa_4Sb_{12}$ through the melting,quenching,annealing,and SPS methods and examine the thermal conductivity and electrical transport properties of $Ba_rIn_sCa_4Sb_{12}$ with in the temperature range of 300-850k.They improved σ by modulation doping method and achieved high ZT values 1.33 and 1.34 at the temperature 850k for $Ba_{0.15}In_{0.16}Ca_4Sb_{11.83}$and$Ba_{0.14}In_{0.23}Co_4Sb_{11.8}$respectively[29].

4. **Thermal Conductivity (*k*):** It explains how efficiently a material can transfer heat in the presence of a temperature gradient.

$$q= -k\nabla T \qquad (23)$$

Where $k$ refers to thermal conductivity ,q refers to heat flux and ∇T refers to temperature gradient [30].In thermoelectrics, thermal conductivity arises from two sources: heat is carried by electrons and holes (e), and phonons travel through the lattice (l). As per the Wiedemann-Franz law, the electronic term (e) is directly associated with electrical conductivity.

$$k = k_e+k_l \qquad (24)$$

$$k_e= L\sigma T = ne\mu LT$$

Where L referred to Lorenz factor,$2.4*10^{-8}J^2K^{-2}C^{-2}$ with regard to free electrons.

- **Measurement of Thermal Conductivity**: For a semiconductor where the heat transfer rate is comparable to that of surrounding environment. Measuring the thermal conductivity is time consuming and difficult due to the Heat exchange[31].One of the best techniques to calculate the thermal conductivity of thermoelectric material is steady state technique . According to the steady state condition,

$$\boldsymbol{k}=(Q_s\backslash A)(\Delta T\backslash \Delta L) \qquad (25)$$

Where A denotes cross section area,$Q_s$ denotes the amount of heat passing through the cross section area per unit time,ΔT denotes the temperature difference and ΔL is the distance over the temperature difference .$Q_s$\A is the heat flux responsible for the production of the temperature difference . ΔT\ΔL Thus, temperature differential and heat flow measurements are necessary in order to determine thermal conductivity[32].

- **Strategy to Reduce the Thermal Conductivity:** Nanostructuring proved effectively in lowering thermal conductivity by incorporating nanoscale heterogeneities and nano dispersions. Energy filtering effects and quantum confinement are observed as the system size reduces, the length scale approaches that of the electron's mean free path or wavelength..This leads to an increase in the density of states (DOS), ultimately boosting the Seebeck coefficient.Conversely, the incorporation of nanostructured surfaces or interfaces causes thermal conductivity to decrease due to the scattering of phonons.The enhancing properties of nanowires,quantum dots, supperlattices, and thin-films are successfully proven by this method.When dealing with bulk materials such as PbTe, LAST, and LASTT, nanoscale impacts can be regulated by either reducing grain size to the nanometer scale or incorporating nanoparticles (NPs). Effectively manipulating nanoscale interfaces within nanostructured materials emerges as a crucial factor in diminishing lattice thermal conductivity. Consequently, leveraging these interfaces has the potential to substantially elevate the ZT, especially in the context of nanostructured materials[33].

  Xiaoming Hu et,al. prepared the Bi0.4Sb1.6Te3 through the zone melting or Bridgeman method and reported an increase in porosity led to a notable decline in both thermal and electrical conductivities. Nevertheless, electrical conductivity reduction was counter balanced by the reduction in thermal conductivity. Resulting, achieved the ZT value 1.1 at 343 K. This represents a significant improvement of about 20% compared to the original dense sample[34].

  Yi Wu et al.,synthesized the n-type polycrystalline $Bi_2S_3$ doped with $Lacl_3$ via the solid-state reaction and spark plasma sintering technique were employed to fabricate a Bi2S3 sample doped with 2 mole% LaCl3. It exhibited a ZT value of 0.5 at 625K, surpassing the 0.11 ZT value observed for pure Bi2S3 at the same temperature.. It is also reported that, at a temperature of 625k,$Bi_2S_3$ sample with 2mole%$LaCl_3$ exhibited the maximum power factor(PF), approximately 483$\mu Wm^{-1}K^{-2}$. The introduction of doping in the sample led to the lattice thermal conductivity reduction , which is attributed to the occurrence of multi-scale phonon scattering[35].

  S. Alagar Nedunchezhian et al., frabricated the $Bi_xCo_{3-x}O_4$ through the chemical precipitation method and reported a high power factor of 0.025$\mu Wm^{-1}K^{-2}$at 530k observed in the $Bi_{0.2}Co_{2.8}O_4$sample and showed that doping in Bi has a favorable impact on improving the $Bi_xCo_{3-x}O_4$ sample thermoelectric properties [36].

5. **Figure of merit (ZT):** In the earlier 19th century,engineers have been working to create an efficient and financial viability TEG. They believed that efficiency of the TEG depends upon the properties of thermoelectric material and construction of TEG. In 1909, a German scientist named Edmund Altenkirch described the mathematical relationship between the TMs physical properties and TEG efficiency .The electromotive force, a thermopile's thermal resistance and electrical conductivity, and other factors are

included in Altenkirch's equation .In 1949 to 1956, these characteristics were merged into the Z group by the renowned Russian scientist Abram F. Ioffe,Researchers utilized the novel parameter Z to evaluate efficiency[37].The efficiency of TMs calculated by dimension less quantity

$$ZT= \frac{S^2\sigma T}{k} = \frac{S^2\sigma T}{k_e+k_l} \qquad (26)$$

Where $S^2\sigma$ is called power factor , seebeck coefficient denoted by S,showed in units of $VK^{-1}$; electrical conductivity denoted by$\sigma$,showed in units of $Scm^{-1}$; absolute temperature denoted by T,expressed in units of K; thermal conductivity denoted by $k$ ,expressed in units of $Wm^{-1}K^{-1}$. The thermal conductivity$k$ is in the terms of elctronic thermal conductivity $k_e$and lattice thermal conductivity $k_l$. .A device with a huge power factor can produce high voltage and current[38].

6. **Maximum Efficiency:** The expression for the thermoelectric efficiency ( Ɛ ) when generating power and coefficient of performance in refrigeration mode for a thermo electric couple are follows

$$Ɛ = Ɛ_c \left[\frac{\sqrt{1+ZT_m}-1}{\sqrt{1+ZT_m}+\frac{T_c}{T_H}}\right] \qquad (27)$$

$$\text{And } \eta = \frac{1}{Ɛ_c}\left[\frac{\sqrt{1+ZT_m}-\frac{T_c}{T_H}}{\sqrt{1+ZT_m}+1}\right] \qquad (28)$$

Where $Ɛ_c$ is the carnot efficiency as follows the

$$Ɛ_c= \frac{T_H - T_c}{T_H} \qquad (29)$$

Where $T_H$ is the hotside of TEG ,$T_c$ is cold side of TEG ,and $T_m$ is average temperature of TEG[39].

To clarify, enhancing the temperature differential across the legs results in an elevation of the conversion efficiency of Thermoelectric Generators. To optimize the Carnot efficiency ($\eta_C$), a highly effective strategy involves adjusting the structural configuration of the Thermoelectric legs in accordance with the ideal proportion of the cross-sectional area of the p-type (Ap) and n-type (An) legs. Determining the optimal ratio can be achieved by evaluating the respective measurements of these cross-sectional areas.

$$\left[\frac{A_n}{A_p}\right] = \sqrt{\frac{\sigma_p \lambda_p}{\sigma_n \lambda_n}} \qquad (30)$$

Where $\sigma_p$ and $\sigma_n$ represents electrical conductivity and $\lambda_p$ ,$\lambda_n$ represents thermal conductivity[40].

7. **Output power of TEG:** The output power (P) is derived as below:

$$P = \frac{V_{TEG}^2}{(R_{TEG} + R_{EL})^2} R_{EL} \qquad (31)$$

Where internal electrical resistance is denoted by $R_{TEG}$ and external electrical resistance is denoted by $R_{EL}$ .If the internal electrical resistance ($R_{TEG}$) is equivalent to the external electrical resistance $R_{EL}$ resulting,maxium power occurs. The output power density measured by the equation

$$E = \frac{P}{S} = \frac{P}{L*W} \qquad (32)$$

Where surface area of the TEG is denoted by S, width of the TEG denoted by W and length of the TEG denoted by L[41].

8. **Applications:** Mainly the thermoelectric devices are classified into the two types, one is thermoelectric generator (TEG) which is used to generate the electricity from the heat. Another one is the thermoelectric cooler (TEC) which is used to convert the electricity to heat. TEG and TEC are using in many areas including space ,automobiles ,electronic devices and buildings etc.,

For many missions exploring different planets, relying on solar power to generate electricity isn't feasible due to the diminishing solar brightness. This is especially true on Mars, where it's only about 45% as bright as in Earth's orbit, less than 4% on Jupiter, and virtually nonexistent farther out. Instead, over the past forty years, missions have utilized radioisotope thermoelectric generators to convert the thermal energy from a radioactive heat source into electricity for power[42]. Since 1961, Radioisotope Thermoelectric Generators (RTGs) have been employed by the United States to provide electrical power for spacecraft missions.RTGs achieve the necessary electrical output by incorporating General-Purpose Heat-Source (GPHS) modules. These modules consist of a composite carbon structure housing four fuel pellets, primarily containing plutonium dioxide (238PuO2) at around 80% density. The RTG system employs thermoelectric junctions, like SiGe junctions, for power conversion[43].

Bombardier submitted a patent outlining a Thermoelectric Generator (TEG) coupled with a latent heat storage unit linked to the TEG's high-temperature end. This storage mechanism aims to reduce the temperature fluctuations commonly experienced in applications like diesel-electric locomotives[44].

9. **Thermoelectric Materials:** There are several categories of materials that have been exhibiting the thermoelectric properties such as polymers, carbon nano materials,inorganic materials etc. Due to the superior thermoelectric properties of inorganic compunds compared to organic made them to use widely .The inorganic compunds are divided into oxides , clathrates , skutterudites, HH alloys, Zinc-phase materials ,intermatallics, and nitrides each with their own unique physical properties,thermoelectric perfomance,and crystal structure

- **Oxides:** Oxides are the well known inorganic materials for the preparation of thermoelectric materials. There is increasing interest in oxides for high temperature uses due to their potential stability and chemical inertness. Yakabeet al.[45] discovered the potential for utilizing them as thermoelements when they observed a significant figure of merit in $NaCo_2O_4$, a material they prepared through sintering, employing both hot and cold pressing methods. The hot pressing material maintained a figure of merit above 0.5□$10^{-3}K^{-1}$ across the 100-400□C temperature range. The Seebeck coefficient ranged from 100to140 □V/K, falling short of the optimal value. Doping agents like Ba, Cu, and Mn were found to enhance the seebeck coefficient, especially the material $Na(Co_{0.95}Cu_{0.05})_2O_4$ displaying the high ZT value 0.8□$10^{-3}K^{-1}$ due to its lower thermal conductivity of about 1.0W/m k from 100to400C. The peak ZT value reached approximately 0.54 at 400°C,This marks a hopeful beginning for further investigation into oxide systems.

  Ohtaki et al. [46] revealed an improvement in the thermoelectric properties of $NaCo_2O_4$ via a crucial double-sintering method. This procedure led to the highest Seebeck coefficient and electrical conductivity, effectively doubling the power factor, albeit starting from a relatively modest level. At 780 °C, the p-type conductor exhibited a ZT value of 0.78, a performance similar to another p-type oxide, $Ca_3Co_4O_9$ [47]. This underscores that $NaCo_2O_4$ is not the sole oxide manifesting noteworthy thermoelectric characteristics.

  The initial materials belonging to Ruddlesden- Popper phase ($Sr3Ti_2O_7$) were reported in 1958[48] whose parent peroviskite is $SrTiO_3$.The significant thermopower value is evident due to the substantial effective mass of the carriers arising from its d-band structure. $SrTiO_3$ is one of the good n-type oxide[49].Despite its low mobility, $SrTiO_3$ boasts a high effective mass, and its power factor at the room temperature competes favorably with materials like $Bi_2Te_3$. Nevertheless, the material's thermal conductivity is relatively high at around 8 W/m K, yielding a modest ZT value of about 0.08 at room temperature. Notably, Muta et al.[50] effectively decreased the thermal conductivity to 3.4 W/m K at 300 K by introducing Dy as a partial substitute for Sr. Furthermore, SrTiO3 with a significant concentration of Nb has attained a promising zT value of 0.37 at 1000K.[51]. Despite this progress, further advancements are necessary to establish a decent n-type oxide at 1000 K. Importantly, $SrTiO_3$'s high melting point of 2080 °C suggests potential applications in environments not suitable for other thermoelectric materials. Enhancing the power factor of the pure $SrTiO_3$ involves doping with Nb, but reaching the optimal Seebeck coefficient is hindered by limitations in the amount of dopant that can be added. Alternatively, adjusting for decreasing or oxygen-deficiency doping helps bring the Seebeck coefficient to the desired value[52]. At 1000 K, the Nb-doped material exhibited a zT value of 0.25. Other oxides, such as co-doped n-type SrTiO3 with La and Y occupying one site and Nb occupying another site., surpass this with a zT above 0.3. Additionally, incorporating $TiB_2$ as a second phase or utilizing n-type materials based on $Ti_2O_3$ yields comparable, albeit slightly inferior, properties.

  Terasaki [53] conducted a study on the transition metal oxides power factor , projecting a broad temperature range with a predicted power factor value of 9 μW/cm $K^2$. The associated Seebeck coefficient magnitude would be around 300 μV/K. When considering a realistic thermal conductivity value of 10 W/m K, the resulting zT is estimated to reach 0.9 at 1000 K.

Zinc oxide (ZnO) stands out as a promising n-type oxide thermoelectric material due to its abundant and cost-effective nature, coupled with a high power factor of approximately 80 μW/mK² at room temperature. However, its elevated thermal conductivity around room temperature (about 40 W/mK) and structural symmetry from the wurtzite-like arrangement make it more suitable for high-temperature applications. The substantial reduction in thermal conductivity to around 5 W/mK at 1000 K is attributed to the pronounced anisotropic thermal expansion.

Efforts to improve the thermoelectric efficiency of ZnO have concentrated on decreasing thermal conductivity while maintaining electronic properties, with the goal of enhancing the dimensionless figure of merit (zT). One effective strategy involves the controlled introduction of a secondary phase, forming nano-precipitates through precise thermal treatment. Despite the complexity of this approach, promising results have been achieved, particularly with Al nanocomposites[54]. The introduction of defects and interfaces in these composites resulted in a notable decrease in thermal conductivity to around 2 W/mK at 1000 K, with minimal impact on electronic properties. This yielded a final zT value of 0.44 at 1000 K.Similarly, the incorporation of polyparaphenylene (PPP) nanoparticles into the $Zn_{1-x}Ni_xO$ matrix yielded a zT of 0.54 at 1173 K[55]. This achievement was credited to a higher power factor and decreased thermal conductivity. Nanostructuring of undoped or doped ZnO has consistently demonstrated the ability to lower the thermal conductivity values as low as 3 $Wm^{-1} K^{-1}$ at room temperature for nanograined ZnO[56]. However, challenges persist, such as the limitation in electrical conductivity (σ), hindering substantial improvements in zT. By combining nanostructure with selective dopiant or co-dopants enabled the achievement of enhanced zT values up to 0.65 at 1247 K[57].

- **Skutterudites:** Skutterudite, a mineral initially found in Skutterud, Norway, possesses 32 atoms per unit cell and showcases a distorted $AB_3$-type cubic perovskite structure [58]. $CoSb_3$, a notable skutterudite, undergoes transformation into a heavily doped semiconductor, particularly in the Co-rich phase, making it viable for high-temperature thermoelectric applications [59]. The void-filling atoms play a crucial role by altering electron concentration and acting as potent phonon-scattering centers, thereby reducing the lattice thermal conductivity [58]. Through substitutions of foreign atoms at Co and Sb sites, such as Fe, Ni, Sn, or Te, can alter the properties of $CoSb_3$ for specific applications [60,61].

Studies have revealed that the $Yb_xCo_4Sb_{12}$ system with incorporating fillers significantly enhances the thermoelectric response, resulting in improved ZT values, indicating its suitability for thermoelectric devices [62,63,64,and 65]. Lattice thermal conductivity reduction without affecting electrical conductivity, as seen in materials like PGEC (Phonon-glass electron-crystal), is caused by the phenomenon known as the 'rattling effect', where guest atoms establish feeble bonds with the host lattice. [66]. Moreover, nanostructuring and reducing grain size have been identified as effective strategies to improve the thermoelectric properties of $CoSb_3$ [67,68]. A thermal conductivity of 1.61 W/m K has been attained for bulk CoSb3, which was fabricated from nanopowder synthesized hydrothermally, employing either spark plasma sintering or hot pressing techniques.[67,69].

$CoSb_3$ stands out as a decent candidate for medium-temperature thermoelectric devices due to its well-balanced mechanical and thermal properties, as supported by various studies [67,61,70].

PGEC materials exhibit a structured, cage-like arrangement at regular intervals, enabling unrestricted electron mobility akin to that of a perfect crystal. However, the incorporation of a sizable, heavier guest atom with weak bonding, referred to as a "rattler," disturbs the oscillations caused by lattice vibrations. This disruption results in a material resembling glass, characterized by diminished thermal conductivity.[71]. Shi et al. conducted research wherein they decreased lattice thermal conductivity by introducing Barium and Ytterbium atoms into the voids of a skutterudite structure. This incorporation led to a broad spectrum of resonant phonon scattering. [72].Shi et al. Reported a ZT value of 1.36 at 527°C with an n-type BaxYbyCo4Sb12 material, while the skutterudite Ba0.08La0.05Yb0.04Co4Sb12, featuring multiple-filled voids, exhibited an even higher ZT of 1.7 at 577°C. The importance of reducing lattice thermal conductivity is underscored, particularly in cases like Ba0.08La0.05Yb0.04Co4Sb12, The effectiveness of multiple fillings of filler atoms is shown to be more effective. The significant rise in the ZT value can be credited to the Spark Plasma Sintering (SPS) technique, which not only enhances the material's microstructure but also ensures a uniform and homogeneous filling of atoms within the voids. Yang and team introduced a filled-skutterudite system labeled as GyM4X12, where G represents a rare earth element, M denotes Co, Rh, or Ir, and X represents Sb, P, or As. Interestingly, multiple-filled skutterudite systems, like Ba0.08Yb0.04La0.05Co4Sb12, exhibited an impressive ZT value of 1.8 at 900 K, setting a new record for skutterudites.[73].

- **Clathrates:** As discussed above, the interaction between structure and chemical composition plays a crucial role to determining the electrical and thermal properties, ultimately influencing the thermoelectric performance of materials. This observation is particularly pertinent in the case of intermetallic clathrates, where the distinct geometric atom’s arrangement directly correlates with unconventional thermal transport characteristics. Moreover, the chemical versatility of these substances leads to a broad range of electrical properties. The word "clathrate" generally describes a mixed group of inclusion compounds characterized with shared structural attribute: a host framework composed of one species capable of Capturing atomic or molecular guests from an alternate source. [74].

  While the term encompasses a wide range of crystalline guest-host solids, clathrate materials relevant to thermoelectric applications represent a more specific subset within this extensive category. The terms "inorganic" and "intermetallic" clathrates are frequently used interchangeably, although not entirely accurately, to characterize Chemical compounds comprising atoms bonded covalently, typically tetrahedrally coordinated, create firm frameworks composed of face-sharing coordination polyhedra capable of accommodating different guest atoms.. The crystallization of clathrate compositions can occur in various structure types, each characterized by distinctive polyhedral cages that geometrically constitute the framework [75, 76, 77, and 78].

Clathrates possess a unique crystal structure resembling a cage, created by guest atoms housed within the lattice, thereby leading to reduced thermal conductivity. These clathrate families tetrahedrally coordinate with elements including elements like Si, Ga, Ge, Al or Sn, constructing an open framework. They fall into categories known as type I (A8E46), type II (A24E136), and type III systems, differentiated by their coordination arrangements. [79,80, and 81]. Type III clathrates, exemplified by Ba8Ga15Ge85, are characterized by covalently bonded Ga–Ge pairs within their structure, with cages housing rattling cations. These cations bond to the anion frameworks consisting of tetrakaidecahedral and dodecahedral polyhedra, producing polyatomic compounds in which one element constructs a cage structure enclosing another. [79, and 81].

Certainly: While clathrates frequently display intricate structures comprising multiple phases, These meterials are having the semiconductor phase which is more adavantageous for the thermoelectric objective[79]. Clathrates display characteristics reminiscent of glasses, and their electronic properties can be adjusted through doping [79, 81, and 82]. Guest atoms within the clathrate structure act as "rattlers" confined within the substrate, Effectively scattering lattice phonons, consequently lowering thermal conductivity[83].nonetheless, The concept of "rattling" is being challenged because of the presence of lattice irregularities and point defects, which also play a role in reducing lattice thermal conductivity.

The crystal Ba8Ga16Ge30, synthesized using the Czochralski processes, exhibited the ZT values 1.35 and 1.63 at the temperatures 627 °C, 827°C respectively [84]. Similarly, successfully decreased the thermal conductivity around0.8 W/m K and achieved the ZT value of 1.25 at 627 °C in $Ba_8Ga_{15}Ge_{85}$ type III clathrates like .[85]. YbxBa8-xGa16Ge30, synthesized by Tang et al. through a combination melting and Spark Plasma Sintering, showcased a 1.1 ZT value. The incorporation of Yb atoms filled the empty spots within Ga and Ge, resulting in an enhanced electrical conductivity. However, this enhancement came at the expense of a reduced lattice thermal conductivity.[82].

Zhang et.al.,investigated how different synthesis process, notably Spark Plasma Sintering, affect the $Ba_8Au_{5.3}Ge_{40.7}$ thermoelectric properties, which was produced by the Bridgman method.$Ba_8Au_{5.3}Ge_{40.7}$ displaying p-type attributes along with low thermal conductivity and a high Seebeck coefficient, The ZT values exhibited improvement, increasing from 0.3 at 227 °C to 0.9 at 407 °C following the implementation of Spark Plasma Sintering (SPS) processing [80]. Toberer et al. observed a remarkably low lattice thermal conductivity of 0.14 W/m K at 727 °C in Ba8Ga16Ge30, despite its relatively moderate ZT value of 0.8[79].

A power factor of 15 μW/cm $K^2$ was attained for the Type I Ba8Ga16Ge30, resulting from cross-substitution of framework elements. This accomplishment is attributed to alterations in carrier scattering mechanisms. Additionally, a ZT value of around 1.2 at 727 °C was documented for a polycrystalline material system composed of Ba8Ni0.31Zn0.52Ga13.06Ge32.2. The substitution of framework elements introduced ionized impurities and lattice defects, leading to phonon scattering [86]. Furthermore, a ZT value of 0.87 at 557 °C was reported for Ba8Ni0.22Zn7.22Ge37.12Sn1.44 synthesized via Ni substitution [87].Sr8Ga16-xGe30-y, produced through a solid-state reaction followed by Spark Plasma Sintering (SPS), exhibited a thermal conductivity of under 1 W/m K at 27 °C. Simultaneously, it displayed an increased power factor of 12 μW/cm $K^2$. Additionally, a correlation was noted, indicating that the power factor rose with a decrease in the Ga/Ge ratio [88].

- **Half-Heusler Compounds:** The Cu2MnAl Heusler alloy, in its basic form exhibits ferromagnetic properties and with a structure where copper atoms arrange in a primitive cubic lattice and in alternate cells, Mn and Al atoms are present. The half-Heusler variant of this alloy retains the same structure, but with a notable difference — half of the copper sites lack atoms. In the case of the half-Heusler compound AgAsMg, it assumes a rock salt structure with magnesium (Mg) and silver (Ag) atoms. Additionally, arsenic (As) atoms, along with either Mg or Ag atoms, form a zinc blende structure. A distinct group of half-Heusler (HH) compounds, characterized by the formula MNiSn, where M can be hydrogen (H), zirconium (Zr), or titanium (Ti), is recognized for its commendable n-type thermoelectric properties. Notably, despite a relatively high lattice thermal conductivity, these compounds demonstrate good thermoelectric behavior.

The cubic structure currently under investigation contains 18 valence electrons and exhibits a complex band structure. The electronic characteristics of this structure are predominantly influenced by the covalent bond in between two elements. These bonding configurations are pivotal in determining phase stability and the formation of a bandgap, as detailed in a prior investigation [89]. Within an HH alloy, the presence of vacant atomic sites can facilitate the emergence of narrow bands, which in turn induce d-orbital hybridization, imparting a semiconducting nature. [90]. Notably, HH alloys typically demonstrate narrow bandgaps falling within the range of 0.1 to 0.3 eV [89,90]. These alloys also exhibited heightened Seebeck coefficients, reaching levels of up to 300 μV/K, along with high electrical conductivity in the range of 103–104 S/cm at room temperature. Nonetheless, their practical applicability is hindered by their relatively elevated thermal conductivity, typically around 10 W/m K. Despite this, HH alloys demonstrate exceptional material characteristics,Examples of their exceptional characteristics include a high melting point ranging from 1100 to 1300 °C and remarkable thermal stability maintained up to 1000 °C, as evidenced in prior research [59, 89, and 91]. The atomic disorder which is present at transition metal sites contributing to a reduced thermal conductivity,The attributed characteristics are due to induced mass fluctuations and strain field effects within half-Heusler alloys [92, and 93].

half-Heusler alloys thermoelctric properties have been studied in depth to enhance their performance, Especially concentrating on ZnNiSn as the most thoroughly researched member[94-97]. Notably, incorporated Sb in TiNiSn alloys have demonstrated impressive power factors, reaching up to 70 μW/cm$K^2$ at 377°C. However, their high thermal conductivity of approximately 10 W/mK limits their overall thermoelectric efficiency, reported ZT value of only 0.45 at 377°C[96,98]. In addressing the thermal conductivity challenges, researchers have explored alternative alloy compositions. For example, Shutoh and Sakurada prepared an alloy of Ti0.5(Zr0.5Hf0.5)0.5NiSn1-ySby, reaching a ZT value of 1.5 at 527°C through synthesis[91].The incorporation of Zr and Hf alongside Ti in this alloy significantly diminished the thermal conductivity to 3.1 W/m K at 527°C, consequently boosting the Seebeck coefficient[91, 99]. Additionally, Hf0.6Zr0.4NiSn0.98Sb0.02 and Hf0.75Zr0.25NiSn0.99Sb0.01 alloys were developed and demonstrated ZT values of 1.0 at 727°C and approximately 1 at 600–700°C, respectively [100]. Moreover Zr0.25Hf0.75NiSn alloys, synthesized through high-energy ball milling and spark plasma sintering (SPS), displayed improved ZT values compared to their bulk forms synthesized via arc melting. These alloys offer simultaneous reductions in thermal conductivity and enhancements in the Seebeck coefficient. Recent investigations have unveiled that the unconventional micro- and nanostructures present in arc-melted solid solutions, exemplified by Ti0.37Zr0.37Hf0.26NiSn, resulted in ZT values of 1 at 452°C and 1.5 at 352°C, due to phonon scattering effects caused by mass and strain fluctuations [101]. In a different context, the lattice thermal conductivity of FeVSb alloys increased with higher Nb content. For example, FeV0.6Nb0.4Sb exhibited a lower lattice thermal conductivity (5.6 W/m K) compared to FeVSb (12.2 W/m K) at room temperature [102]. These findings underscore the importance of alloy composition and processing techniques in tailoring thermoelectric properties for optimal performance.

As per Makongo et al., the responsiveness of electrical conductivity, thermal conductivity, and carrier mobility in materials is intricately associated with key parameters such as synthesis methods, processing circumstances, and microstructural characteristics[103]. In mechanically alloyed samples, a notable finding was that a grain size decreasing,led to a notable decrease in both carrier mobility and lattice thermal conductivity.Conversely, in samples processed via Spark Plasma Sintering (SPS), grain growth was noted, resulting in reduced lattice thermal conductivity and moderate carrier mobility [103]. Effective nanostructuring techniques, including ball milling and High-Pressure methods, demonstrated their ability to enhance the ZT value up to 1 at 600–700 °C for n-type $Hf_{0.75}Zr_{0.25}NiSn_{0.99}Sb_{0.01}$ half-Heusler alloys, with grain sizes below 100 nm contributing to further improvements [104].Yan et al. recorded a substantial 60% increase in ZT for p-type half-Heusler (HH) nanopowder produced through ball milling and high pressing[105]. Moreover, introducing excess Ni into TiNi1+xSn (x = 0–0.15) using microwave-assisted techniques, followed by Spark Plasma Sintering (SPS) processes, resulted in decreased thermal conductivity and an enhanced power factor [106].

Chen et al. successfully synthesized a nanocomposite through spark plasma sintering (SPS).In this case, nanophase inclusions of ZrO2 were evenly distributed within the matrix of $Zr_{0.5}Hf_{0.5}Ni_{0.8}Pd_{0.2}Sn_{0.99}Sb_{0.01}$ [107]. The nanocomposite displayed a reduced thermal conductivity, attributed to the phonon scattering effect caused by aggregated ZrO2 nanoparticles at the grain boundaries, acting as efficient scattering sites for phonons[107]. On the contrary, the Seebeck coefficient and electrical resistivity were observed to escalate as a result of potential barrier scattering. Another study has been involved in the grain refinement and the incorporation of nanoparticles in n-type $Hf_{0.6}Zr_{0.4}NiSn_{0.995}Sb_{0.005}$ and p-type $Hf_{0.3}Zr_{0.7}CoSn_{0.3}Sb_{0.7}$/nano-$ZrO_2$ composites and resulting materials displayed the enhanced ZT values of 1.05 and 0.8 at temperatures of 627 and 727 °C, respectively [108]. By employing the atomic-scale structural engineering of thermoelectric (ASSET) approach, simultaneous improvements in thermopower and electrical conductivity were achieved in bulk half-Heusler (HH) alloys integrated with Hf inclusions.The successful application of this approach was evident in $(1-x)Zr_zHf_{1-z}NiSn_{1-y}Sb_y+xZr_zHf_{1-z}Ni_2Sn_{1-y}Bi_y$ nanocomposites, where x is from 0 to 0.1. This approach resulted in an increase in the power factor from 10 to 47 µW/K$^2$, observed within the temperature range of 454 to 527 °C [109]. Sahoo et al. prepared a bulk half-Heusler (HH) matrix of $Ti_{0.5}Hf_{0.5}CoSb_{0.9}Sn_{0.1}$ incorporated with different mole fractions of Hf through solid-state reactions. This investigation underscored the efficacy of this approach in enhancing the thermopower while mitigating the decline in electrical conductivity.The hole-culling effect observed in heavily doped HH alloys tuned the mobility without affecting thermal conductivity, leading to an improve in the Seebeck coefficient [110]. Multiatom substitution in half-Heusler (HH) alloys has been recognized as a more effective strategy for enhancing thermoelectric properties. The multiatom-filled half-Heusler (HH) alloys achieved the highest power factors at 427°C,where multiatom filling and high-temperature annealing notably reduced thermal conductivity while enhancing electrical properties, leading to elevated ZT values [111]. Moving forward, Anticipated future advancements, such as nanostructuring and bandgap engineering, are poised to further refine the thermoelectric characteristics of half-Heusler (HH) alloys. These developments hold the potential to yield ZT values surpassing 2..

- **Zintl-Phase Materials:** Zintl phases, a distinct class of intermetallic compounds composed of electropositive cations primarily sourced from group 1 alkali metals, group 2 alkaline earth metals, and post-transition metals or metalloids from groups 13, 14, 15, or 16, have garnered interest in the realm of thermoelectrics. Although the exploration of their structure and chemical bonding commenced in the 1920s, credit for their discovery goes to German chemist Eduard Zintl, with the term "Zintl phases" coined by Laves in 1941 [112]. These compounds exhibited the promising thermoelectric properties, including high thermopower (S). Notably, $Yb_{2-x}Eu_xCdSb_2$ boasts the highest S value of 269 µVK$^{-1}$ [113], while $Mg_3Pb_{0.2}Sb_{1.8}$ and $Yb_{14}MgSb_{11}$ have also demonstrated S values of approximately 280 µVK$^{-1}$ [114][115]. One notable advantage of Zintl phases is their versatility across a wide temperature range, within the low-to-middle temperature range, Zintl 1-2-2 compounds distinguish themselves by exhibiting superior properties among both p-type and n-type Zintl phases. Conversely, in the high-temperature range, typically between (975-1275) K, the Zintl 14-1-11 compounds outperform other p-type Zintl families [116]. This adaptability renders Zintl phases a promising class of materials for thermoelectric applications.

To attain a high thermoelectric figure of merit (zT), the requisite materials typically possess light carrier effective mass and high band degeneracy [117]. Additionally, they feature small deformation potentials.(resulting in reduced electron-phonon scattering) [118], and low phonon/lattice contribution to the thermal conductivity($\kappa$ph) resembling that of glass. As mentioned earlier, many Zintl compounds have explored due to their intrinsically low κph and exceptional stability at high temperatures, capitalizing on the temperature component (T) in the zT equation. The frequently observed low κph (phonon thermal conductivity) in Zintl phases is frequently attributed to their large unit cells[119]. This is due to the resulting complex phonon dispersions, low average group velocity, and numerous channels for phonon-phonon scattering. However, recent instances of low κph (1.5 W $m^{-1}$ $K^{-1}$) in relatively simple compounds like $Mg_3Sb_2$ [120], adopting the $CaAl_2Si_2$ structure type with only 5 atoms per unit cell, challenge this simple explanation. Despite their lower density [121], $Mg_3Sb_2$ and $Mg_3Bi_2$ exhibit much lower κph than other compounds with the same structure type.This unusual behavior is associated with highly anharmonic bonding, a consequence of the undersized Mg cations in the octahedral site, which leads to weak and unstable interlayer bonding [120,121].

In the realm of Zintl phases, the primary impediment to achieving elevated thermoelectric figure of merit (zT) typically arises from electronic considerations. The majority of thermoelectric Zintl phases reported thus far are of p-type, and Improving the optimization of p-type carrier concentration is typically straightforward.P-type doping can be achieved through either aliovalent doping, such as incorporating $Mn^{2+}$ on the $Al^{3+}$ site in $Yb_{14}MnSb_{11}$ or $Zn^{2+}$ on the $In^{3+}$ site in $Ca_5In_2Sb_6$ [122], or by leveraging intrinsic acceptor-type defects [123]. For example, optimizing zT has been accomplished by alloying with isoelectronic elements on the A site in $A_{1-x}Zn_2Sb_2$ compounds,thereby controlling vacancy concentration [124]. Regrettably, low mobility is a prevalent characteristic of p-type Zintl phases, a quality that can be partially ascribed to their salt-like, ionic nature. To assess the degree of the salt-like nature of a particular $A_aM_mX_x$ compound, the ratio of cations to anions, represented by a/(m + x), is considered, and The evaluation of bond polarity within the polyanion involves considering the difference in electronegativity ($\chi X$ - $\chi M$) between the anions M and X. Using these simple indicators, it has been noted that the intrinsic mobility of Zintl thermoelectrics, evaluated through high-temperature Hall mobility data within a single-band model, tends to decrease in the more salt-like, ionic compounds.

The electronic mobility of compounds, especially in lower temperature ranges, can be impacted by factors like air sensitivity and the inclination to develop resistive phases at grain boundaries. This phenomenon results in low mobility and conductivity (σ) at room temperature and observed to be increase as temperature rises. A comparative study between large-grained (5–20 μm) and small-grained (0.5–2 μm) $Mg_3Sb_2$ samples [125] revealed the similar behavior. Comparable trends have also been documented in various other Zintl phases, including $Ca_3AlSb_3$, $Sr_3GaSb_3$, and $YbZn2Sb_2$ [126, and 127].The obstacle posed by low mobility due to grain boundary resistance is not necessarily innate; instead, it's a challenge that can frequently be addressed through adjustments in processing techniques. These adjustments have the potential to significantly improve the average thermoelectric figure of merit (zT) [126,and 127].

In a recent comprehensive study carried out by Ortiz et al., the results suggest a widespread inclination towards electron transport rather than hole transport in most identified Zintl phases. This tendency is mainly ascribed to the lighter band mass present in the conduction bands [128,129]. Even though Zintl phases inherently tend to develop acceptor-type defects, as demonstrated by Lasse et al[130], the achievement of n-type doping has been limited to a specific set of compounds [131]. Tamaki et al. emphasized the significance of controlling defect formation enthalpies through synthesis condition modifications. Specifically, They conducted a comparison of the formation energies of Mg interstitials (Mgi), Mg vacancies (VMg(1) and VMg(2)), and Te on the Sb site (TeSb) in both Mg-excess and Mg-deficient synthesis conditions. Employing excess Mg during synthesis was discovered to promote n-type doping with Te on the Sb site, leading to the highest reported zT values among all Zintl phases.Remarkably, Te-doped Mg3Sb1.5Bi0.5 exhibited an outstanding zT value of 1.6, a thermal conductivity (κph) of 0.8, and a power factor (PF) of 12 μW $cm^{-1}$ $K^{-1}$. [132]. This successful strategy of excess Mg during synthesis holds promise for enhancing the thermoelectric performance of other Zintl phases. Consequently, while Zintl phases have traditionally been recognized for their p-type, high-temperature thermoelectric capabilities, recent results challenge these expectations and underscore the potential for significant advances in n-type doping [132].

## IV. CONCLUSION

This book chapter presents the overall review on historical background , principles involving in thermoelectric materials,enhancing techniques of ZT and properties of some thermoelectric materials .In a late 18th century volta reviled the concept of thermoelectricity . In 1821 Seebeck discovered phenomena of thermoelectricity is due to the temperature difference in material.In 1834, Peltier discovered the reverse phenomena of Seebeck effect .In 1854 ,the relation between the Seebeck and Peltier coefficients given by Thomson.Ioffe used the parameter ZT to determine the efficiency of TEM. There are some parameters which are contributing to ZT such as electrical conductivity,thermal conductivity and Seebeck coefficient.In this book chapter successfully explained measuring techniques of electrical conductivity by bipolar technique,thermal conductivity by Steady state technique and Seebeck coefficient by Integral method and explained improving strategies of electrical conductivity by Modulation-doping and electron filtering , Seebeck coefficient by Quantum confinement and explained the reduction strategy of thermal conductivity by nano structuring. This chapter reveled some other parameters maximum efficiency of TEG , output power of TEG as well as applications.

## REFERENCES

[1] Bharti, Meetu, Ajay Singh, Soumen Samanta, and D. K. Aswal. "Conductive polymers for thermoelectric power generation." *Progress in Materials Science* 93 (2018): 270-310.

[2] Elsheikh, Mohamed Hamid, Dhafer Abdulameer Shnawah, Mohd Faizul Mohd Sabri, Suhana Binti Mohd Said, Masjuki Haji Hassan, Mohamed Bashir Ali Bashir, and Mahazani Mohamad. "A review on thermoelectric renewable energy: Principle parameters that affect their performance." *Renewable and sustainable energy reviews* 30 (2014): 337-355.

[3] Zulkepli, Nurkhaizan, Jumril Yunas, Mohd Ambri Mohamed, and Azrul Azlan Hamzah. "Review of thermoelectric generators at low operating temperatures: working principles and materials." *Micromachines* 12, no. 7 (2021): 734.

[4] Beretta, Davide, Neophytos Neophytou, James M. Hodges, Mercouri G. Kanatzidis, Dario Narducci, Marisol Martin-Gonzalez, Matt Beekman et al. "Thermoelectrics: From history, a window to the future." *Materials Science and Engineering: R: Reports* 138 (2019): 100501.

[5] Doms, Inge, Patrick Merken, and Chris Van Hoof. "Comparison of DC-DC-converter architectures of power management circuits for thermoelectric generators." In *2007 European Conference on Power Electronics and Applications*, pp. 1-5. IEEE, 2007.

[6] Zhao, Wenrui, Jiamin Ding, Ye Zou, Chong-an Di, and Daoben Zhu. "Chemical doping of organic semiconductors for thermoelectric applications." *Chemical Society Reviews* 49, no. 20 (2020): 7210-7228.

[7] Shittu, Samson, Guiqiang Li, Xudong Zhao, and Xiaoli Ma. "Review of thermoelectric geometry and structure optimization for performance enhancement." *Applied Energy* 268 (2020): 115075.

[8] Gao, H. B., G. H. Huang, H. J. Li, Z. G. Qu, and Y. J. Zhang. "Development of stove-powered thermoelectric generators: A review." *Applied Thermal Engineering* 96 (2016): 297-310.

[9] Sharma, Sudhanshu, V. K. Dwivedi, and S. N. Pandit. "A review of thermoelectric devices for cooling applications." *International journal of green energy* 11, no. 9 (2014): 899-909.

[10] Handbook, Thermoelectrics. "Macro to Nano, edited by DM Rowe." *CRC Taylor & Francis, Boca Ratcon* (2006).

[11] Goldsmid, H. Julian. *Introduction to thermoelectricity*. Vol. 121. Berlin: Springer, 2010.

[12] Lee, HoSung. "The Thomson effect and the ideal equation on thermoelectric coolers." *Energy* 56 (2013): 61-69.

[13] Brostow, Witold, Gregory Granowski, Nathalie Hnatchuk, Jeff Sharp, and John B. White. "Thermoelectric phenomena." *J. Mater. Ed* 36 (2014): 175-185.

[14] Dehkordi, Arash Mehdizadeh, Mona Zebarjadi, Jian He, and Terry M. Tritt. "Thermoelectric power factor: Enhancement mechanisms and strategies for higher performance thermoelectric materials." *Materials Science and Engineering: R: Reports* 97 (2015): 1-22.

[15] Wang, Chen, Fenggui Chen, Kuan Sun, Rui Chen, Meng Li, Xiaoyuan Zhou, Yuyang Sun, Dongyang Chen, and Guoyu Wang. "Contributed Review: Instruments for measuring Seebeck coefficient of thin film thermoelectric materials: A mini-review." *Review of Scientific Instruments* 89, no. 10 (2018).

[16] Ma, Zhe, Jiangtao Wei, Peishuai Song, Mingliang Zhang, Liangliang Yang, Jing Ma, Wen Liu, Fuhua Yang, and Xiaodong Wang. "Review of experimental approaches for improving zT of thermoelectric materials." *Materials Science in Semiconductor Processing* 121 (2021): 105303.

[17] Martin, Joshua, Terry Tritt, and Ctirad Uher. "High temperature Seebeck coefficient metrology." *Journal of Applied Physics* 108, no. 12 (2010).

[18] Amagai, Y., T. Shimazaki, K. Okawa, H. Fujiki, T. Kawae, and N-H. Kaneko. "Precise measurement of absolute Seebeck coefficient from Thomson effect using ac-dc technique." *AIP Advances* 9, no. 6 (2019).

[19] Mao, Jun, Zihang Liu, and Zhifeng Ren. "Size effect in thermoelectric materials." *npj Quantum Materials* 1, no. 1 (2016): 1-9.

[20] Dresselhaus, M. S., G. Dresselhaus, X. Sun, Z. Zhang, S. B. Cronin, and T. Koga. "Low-dimensional thermoelectric materials." *Physics of the Solid State* 41 (1999): 679-682.

[21] Li, Cuncheng, Shifang Ma, Ping Wei, Wanting Zhu, Xiaolei Nie, Xiahan Sang, Zhigang Sun, Qingjie Zhang, and Wenyu Zhao. "Magnetism-induced huge enhancement of the room-temperature thermoelectric and cooling performance of p-type BiSbTe alloys." *Energy & Environmental Science* 13, no. 2 (2020): 535-544.

[22] Hung, Nguyen T., Ahmad RT Nugraha, Eddwi H. Hasdeo, Mildred S. Dresselhaus, and Riichiro Saito. "Diameter dependence of thermoelectric power of semiconducting carbon nanotubes." *Physical review B* 92, no. 16 (2015): 165426.

[23] Goldsmid, H. J. "The electrical conductivity and thermoelectric power of bismuth telluride." *Proceedings of the Physical Society* 71, no. 4 (1958): 633.

[24] Martin, Joshua, and George S. Nolas. "Apparatus for the measurement of electrical resistivity, Seebeck coefficient, and thermal conductivity of thermoelectric materials between 300 K and 12 K." *Review of Scientific Instruments* 87, no. 1 (2016).

[25] Dehkordi, Arash Mehdizadeh, Mona Zebarjadi, Jian He, and Terry M. Tritt. "Thermoelectric power factor: Enhancement mechanisms and strategies for higher performance thermoelectric materials." *Materials Science and Engineering: R: Reports* 97 (2015): 1-22.

[26] Gayner, Chhatrasal, and Yaron Amouyal. "Energy filtering of charge carriers: current trends, challenges, and prospects for thermoelectric materials." *Advanced Functional Materials* 30, no. 18 (2020): 1901789.

[27] Zhu, Qiang, Suxi Wang, Xizu Wang, Ady Suwardi, Ming Hui Chua, Xiang Yun Debbie Soo, and Jianwei Xu. "Bottom-up engineering strategies for high-performance thermoelectric materials." *Nano-Micro Letters* 13, no. 1 (2021): 119.

[28] Tan, Qing, Li-Dong Zhao, Jing-Feng Li, Chao-Feng Wu, Tian-Ran Wei, Zhi-Bo Xing, and Mercouri G. Kanatzidis. "Thermoelectrics with earth abundant elements: low thermal conductivity and high thermopower in doped SnS." *Journal of Materials Chemistry A* 2, no. 41 (2014): 17302-17306.

[29] Zhao, Wenyu, Ping Wei, Qingjie Zhang, Chunlei Dong, Lisheng Liu, and Xinfeng Tang. "Enhanced thermoelectric performance in barium and indium double-filled skutterudite bulk materials via orbital

hybridization induced by indium filler." *Journal of the American Chemical Society* 131, no. 10 (2009): 3713-3720.
[30] Kraemer, D., and G. Chen. "A simple differential steady-state method to measure the thermal conductivity of solid bulk materials with high accuracy." *Review of Scientific Instruments* 85, no. 2 (2014).
[31] Kavei, G., Y. Zare, and A. Seyyedi. "Tentative design for measurements of absolute value of thermal conductivity of semi-conducting thermoelectric elements." *Material Science Research of India* 5, no. 1 (2008): 43-48.
[32] Dasgupta, T., and A. M. Umarji. "Apparatus to measure high-temperature thermal conductivity and thermoelectric power of small specimens." *Review of scientific instruments* 76, no. 9 (2005).
[33] Gayner, Chhatrasal, and Kamal K. Kar. "Recent advances in thermoelectric materials." *Progress in Materials Science* 83 (2016): 330-382.
[34] Hu, Xiaoming, Jie Hu, Bo Feng, Zhao Pan, Peihai Liu, Yanglin Zhang, Rusong Li, Zhu He, Guangqiang Li, and Yawei Li. "Artificial porous structure: An effective method to improve thermoelectric performance of Bi2Te3 based alloys." *Journal of Solid State Chemistry* 282 (2020): 121060.
[35] Wu, Yi, Qing Lou, Yang Qiu, Jun Guo, Zhi-Yuan Mei, Xiao Xu, Jing Feng, Jiaqing He, and Zhen-Hua Ge. "Highly enhanced thermoelectric properties of nanostructured Bi 2 S 3 bulk materials via carrier modification and multi-scale phonon scattering." *Inorganic Chemistry Frontiers* 6, no. 6 (2019): 1374-1381.
[36] Nedunchezhian, AS Alagar, D. Sidharth, N. Yalini Devi, R. Rajkumar, P. Rajasekaran, M. Arivanandhan, G. Anbalagan, and R. Jayavel. "Effect of Bismuth substitution on the enhancement of thermoelectric power factor of nanostructured BixCo3-xO4." *Ceramics International* 45, no. 6 (2019): 6782-6787.
[37] Polozine, Alexandre, Susanna Sirotinskaya, and Lírio Schaeffer. "History of development of thermoelectric materials for electric power generation and criteria of their quality." *Materials Research* 17 (2014): 1260-1267.
[38] Ma, Zhe, Jiangtao Wei, Peishuai Song, Mingliang Zhang, Liangliang Yang, Jing Ma, Wen Liu, Fuhua Yang, and Xiaodong Wang. "Review of experimental approaches for improving zT of thermoelectric materials." *Materials Science in Semiconductor Processing* 121 (2021): 105303.
[39] Chen, Zhi-Gang, Guang Han, Lei Yang, Lina Cheng, and Jin Zou. "Nanostructured thermoelectric materials: Current research and future challenge." *Progress in Natural Science: Materials International* 22, no. 6 (2012): 535-549.
[40] Soleimani, Zohreh, Stamatis Zoras, Boris Ceranic, Yuanlong Cui, and Sally Shahzad. "A comprehensive review on the output voltage/power of wearable thermoelectric generators concerning their geometry and thermoelectric materials." *Nano Energy* 89 (2021): 106325.
[41] Du, Yong, Jiayue Xu, Biplab Paul, and Per Eklund. "Flexible thermoelectric materials and devices." *Applied Materials Today* 12 (2018): 366-388.
[42] He, Wei, Gan Zhang, Xingxing Zhang, Jie Ji, Guiqiang Li, and Xudong Zhao. "Recent development and application of thermoelectric generator and cooler." *Applied Energy* 143 (2015): 1-25.
[43] Rinehart, Gary H. "Design characteristics and fabrication of radioisotope heat sources for space missions." *Progress in Nuclear Energy* 39, no. 3-4 (2001): 305-319.
[44] Champier, Daniel. "Thermoelectric generators: A review of applications." *Energy Conversion and Management* 140 (2017): 167-181.
[45] H. Yakabe, K. Kikuchi, I. Terasaki, Y. Sasago, K. Uchinokura, in Proceedings of the Sixteenth International Conference on Thermoelectrics, Dresden (IEEE, New York, 1997), p. 523.
[46] M. Ohtaki, Y. Nojiri, E. Maeda, in Proceedings of the Nineteenth International Conference on Thermoelectrics, Cardiff (Babrow Press, Wales, 1997), p. 190.
[47] H. Ohta, K. Sugiura, K. Koumoto, Inorganic Chem. 47, 8429 (2008).
[48] S.N. Ruddlesden, P. Popper, Acta Crystallogr. 11 (1958) 54–55.
[49] K.K. Koumoto, I. Terasaki, T. Kajitani, M. Ohtaki, R. Funahashi, Thermoelectrics Handbook: Macro to Nano, ed. by D.M. Rowe (CRC Taylor and Francis, Boca Raton, 2006), p. 35-1
[50] H. Muta, K. Kurosaki, S. Yamanaka, J. Alloy. Compd. 350, 292 (2003)
[51] S. Ohta, T. Nomura, H. Ohta, M. Hirano, H. Hosono, K. Koumoto, Appl. Phys. Lett. 87, 092108 (2005)
[52] M. Backhaus-Ricoult, J. Rustad, L. Moore, C. Smith, J. Brown, Appl. Phys. A 116, 433 (2014)
[53] I. Terasaki, J. Appl. Phys. 110, 053705 (2011).
[54] P. Jood, R.J. Mehta, Y. Zhang, G. Peleckis, X. Wang, R.W. Siegel, T. Borca-Tasciuc, S.X. Dou, G. Ramanath, Nano Lett. 11 (2011) 4337–4342.
[55] Z.-H. Wu, H.-Q. Xie, Y.-B. Zhai, Appl. Phys. Lett. 103 (2013) 243901.
[56] M. Ohtaki, K. Araki, K. Yamamoto, J. Electron. Mater. 38 (2009) 1234–1238.

[57] H. Shirakawa, E.J. Louis, A.G. MacDiarmid, C.K. Chiang, A.J. Heeger, J. Chem. Soc. Chem. Commun. 0 (1977) 578.
[58] Nolas GS, Morel DT, Tritt TM. Skutterudites: a phonon-glass-electron crystal approach to advance thermoelectric energy conversion application. Ann Rev Mater Sci 1999;29:89–116.
[59] Sootsman JR, Chung DY, Kanatzidis MG. New and old concepts in thermoelectric materials. Angew Chem Int Ed 2009;48:8616–39.
[60] Leszczynski J, Wojeciechowski KT, Malecki AL. Studies on thermal decomposition and oxidation of CoSb3. J Therm Anal Calorim 2011;105:211–22.
[61] Liu WS, Zhang B, Li JF, Zhao L. Effects of Sb compensation on microstructure, thermoelectric properties and point defect of CoSb3 compound. J Phys D: Appl Phys 2007;40:6784–90.
[62] Nolas GS, Kaeser M, Littleton RT, Tritt TM. High figure of merit in partially filled ytterbium skutterudite materials. Appl Phys Lett 2000;77:1855–7.
[63] Shi X, Yang J, Salvador JR, Chi M, Chao JY, Wang H, et al. Multiple-filled skuttelluride: high thermoelectric figure of merit through separately optimising electrical and thermal transport. J Am Chem Soc 2011;133:7837–46.
[64] Ballikaya S, Wang G, Sun K, Uher C. Thermoelectric properties of triple-filled $Ba_xYb_yIn_zCo_4Sb_{12}$ skutterudites. J Electron Mater 2011;40:570–6.
[65] Graff J, Zhu S, Holgate T, Peng J, He J, Tritt TM. High temperature thermoelectric properties of $Co_4Sb_{12}$ based skutterudites with multiple filler atoms: Ce0.1InxYbyCo4Sb12. J Electron Mater 2011;40:696–701.
[66] Slack GA, Tsoukala VG. Some properties of semiconducting $IrSb_3$. J Appl Phys 1994;76:1665–71.
[67] Mi JL, Zhu TJ, Zhao XB, Ma J. Nanostructuring and thermoelectric properties of bulk skutterudite compound $CoSb_3$. J Appl Phys 2007;101. 054314(1–6).
[68] Toprak MS, Stiewe C, Platzek D, Williams S, Bertini L, Muller E, et al. The impact of nanostructuring on the thermal conductivity of thermoelectric $CoSb_3$. Adv Funct Mater 2004;14:1189–96.
[69] Li JF, Liu WS, Zhao LD, Zhau M. High performance nanostructured thermoelectric materials. NPG Asia Mater 2010;2:152–8.
[70] Goldsmith HJ. Introduction to thermoelectricity. Heidelberg: Springer; 2010.
[71] Graff J, Zhu S, Holgate T, Peng J, He J, Tritt TM. High temperature thermoelectric properties of $Co_4Sb_{12}$ based skutterudites with multiple filler atoms: $Ce_{0.1}In_xYb_yCo_4Sb_{12}$. J Electron Mater 2011;40:696–701.
[72] Shi X, Kong H, Li CP, Uher C, Yang J, Salvador JR, et al. Low thermal conductivity and high thermoelectric figure of merit in n-type $Ba_xYb_yCo_4Sb_{12}$ double-filled skutterudite. J Phys Lett 2008;92. 182101(1–3).
[73] Yang J, Shi X, Bai S, Zhang W, Chen L. Thermoelectric material including a filled skutterudite crystal structure. US patent 0071741 A1, 2010 March 25.
[74] in:, IUPAC Compend. Chem. Terminol., IUPAC, Research Triagle Park, NC, n.d.
[75] D.M. Rowe, Thermoelectrics Handbook: Macro to Nano, CRC/Taylor & Francis, Boca Raton, 2006.
[76] A.V. Shevelkov, K. Kovnir, T.F. Fässler (Ed.), Zintl Phases Princ. Recent Dev. Springer Berlin Heidelberg, Berlin, Heidelberg, 2011, pp. 97–142.
[77] G.S. Nolas, G.A. Slack, S.B. Schujman, Semicond. Semimetals 69 (2001) 255–300.
[78] P. Rogl, D.M. Rowe (Ed.), Thermoelectrics Handbook: Macro to Nano, CRC Press, 200632-1.
[79] Toberer E, Christensen M, Iversen BB, Snyder GJ. High temperature thermoelectric efficiency in $Ba_8Ga_{16}Ge_{30}$. Phys Rev B 2008;77. 075203(1–8).
[80] Zhang H, Borrmann H, Oeschler N, Candolfi C, Schelle W, Schmidt M, et al. Atomic interaction in the p-type clathrate I $Ba_8Au_{5.3}Ge_{40.7}$. Inorg Chem 2011;50:1250–7.
[81] Kleinke H. New bulk materials for thermoelectric power generation: clathrates and complex antimonides. Chem Mater 2010;22:604–11.
[82] Tang X, Li P, Deng S, Zhang Q. High temperature thermoelectric transport properties of double atom filled clathrates compounds $Yb_xBa_{8-x}Ga_{16}Ge_{30}$. J Appl Phys 2008;104. 013706(1–6).
[83] Nolas GS, Slack GA, Schujman SB. Semiconductor clathrates: a phonon glass crystal material with potential for thermoelectric application. In: Tritt TM, editor. Recent trends in thermoelectric materials research I – semiconductor and semimetals. London: Academic press; 2001.
[84] Saramat A, Svensson G, Palmavist AE, Stiewe C, Mueller E, Platzek D, et al. Large thermoelectric figure of merit at high temperature in czochralski grown clathrates $Ba_8Ga_{16}Ge_{30}$. J Appl Phys 2006;99. 023708(1–5).
[85] Kim JH, Okamoto NL, Kishida K, Tanaka K, Inui H. High thermoelectric performance of type-III clathrate compounds of the Ba-Ge-Ga system. Acta Mater 2006;54:2057–62.

[86] Shi BX, Yang J, Bai S, Yang J, Wang H, Chi M, et al. On the design of high-efficiency thermoelectric clathrates through a systematic cross-substitution of framework elements. Adv Funct Mater 2010;20:755–63.
[87] Falmbigl M, Grytsiv A, Rogl P, Heinrich P, Royanian E, Bauer E. Tuning of band gap and thermoelectric properties of type-I clathrate $Ba_8Ni_xZn_yGe_{46-x-y-z}Sn_z$. J Alloys Compd 2013;567:65–72.
[88] Wang L, Chen LD, Chen XH, Zhang WB. Synthesis and thermoelectric properties of n-type $Sr_8Ga_{16-x}Ge_{30-y}$ clathrates with different Ga/Ge ratios. J Phys D: Appl Phys 2009;42. 045113(1–6).
[89] Poon SJ. Electronic and thermoelectric properties of half-Heusler alloys. In: Tritt TM, editor. Recent trends in thermoelectric materials research II–semiconductor and semimetals. London: Academic press; 2001.
[90] Graf T, Felser C, Parkin SSP. Simple rules for the understanding of Heusler compounds. Prog Solid State Chem 2011;39:1–50.
[91] Shutoh N, Sakurada S. Thermoelectric properties of the $Ti_x(Zr_{0.5}Hf_{0.1})_{1-x}NiSn$ half Heusler compounds. J Alloys Compd 2005;389:204–8.
[92] Yang J, Li H, Wu T, Zhang W, Chen L, Yang J. Evaluation of half Heusler compound as thermoelectric materials based on the calculated electrical transport properties. Adv Funct Mater 2008;18:2880–8.
[93] Shen Q, Chen L, Goto T, Hirai T, Yang J, Meisner GP, et al. Effects of partial substitution of Ni by Pd on the thermoelectric properties of ZrNiSn-based half Heusler compounds. Appl Phys Lett 2001;79(25):4165–71.
[94] C. Uher, J. Yang, S. Hu, D. T. Morelli, G. P. Meisner, Phys. Rev. B 1999, 59, 8615.
[95] Y. Xia, S. Bhattacharya, V. Ponnambalam, A. L. Pope, S. J. Poon, T. M. Tritt, J. Appl. Phys. 2000, 88, 1952.
[96] S. Bhattacharya, A. L. Pope, R. T. Littleton IV, T. M. Tritt, V. Ponnambalam, Y. Xia, S. J. Poon, Appl. Phys. Lett. 2000, 77, 2476.
[97] H. Hohl, A. P. Ramirez, C. Goldmann, G. Ernst, B. Wolfing, E. Bucher, J. Phys. Condens. Matter 1999, 11, 1697.
[98] Bhattacharya S, Pope AL, Littleton RT, Tritt TM, Ponnambalam V, Xia Y, et al. Effect of Sb doping on the thermoelectric properties of Ti based half Heusler compounds, TiNiSn1xSbx. Appl Phys Lett 2000;77(16):2476–8.
[99] Sakurada S, Shutoh N. Effect of Ti substitution on the thermoelectric properties of (Zr, Hf)NiSn half-Heusler compounds. Appl Phys Lett 2005;86. 082105 (1–3).
[100] Chen S, Lukas KC, Liu W, Opeil CP, Chen G, Ren Z. Effect of Hf concentration on thermoelectric properties of nanostructured n-type half-Heusler materials $Hf_xZr_{1-x}NiSn_{0.99}Sb_{0.01}$. Adv Energy Mater 2013;3:1210–4.
[101] Populoh S, Aguirre MH, Brunko OC, Galazka K, Lu Y, Weidenkaff A. High figure of merit in (Ti, Zr, Hf)NiSn half-Heusler alloys. Scr Mater 2012;66:1073–6.
[102] Fu C, Xie H, Zhu TJ, Xie J, Zhao XB. Enhanced phonon scattering by mass and strain field fluctuations in Nb substituted FeVSb half-Heusler thermoelectric materials. J Appl Phys 2012;112. 124915 (1–5).
[103] Makongo JPA, Zhou X, Misra DK, Uher C, Poudeu Pierre FP. Correlation between processing conditions, microstructure and charge transport in halfHeusler alloys. J Solid State Chem 2013;201:280–7.
[104] Joshi G, Yan X, Wang H, Liu W, Chen G, Ren Z. Enhancement in thermoelectric figure of merit of an n-type half-Heusler compound by the nanocomposite approach. Adv Energy Mater 2011;1:643–7.
[105] Yan X, Joshi G, Liu W, Lan Y, Wang H, Lee S, et al. Enhanced thermoelectric figure of merit of p-type half-Heuslers. Nano Lett 2011;11:556–60.
[106] Birkel CS, Douglas JE, Lettiere BR, Seward G, Verma N, Zhang Y, et al. Improving the thermoelectric properties of half-Heusler TiNiSn through inclusion of a second full-Heusler phase: microwave preparation and spark plasma sintering of $TiNi_{1+x}Sn$. Phys Chem Chem Phys 2013;15:6990–7.
[107] Chen LD, Huang XY, Zhou M, Shi X, Zhang WB. The high thermoelectric performances of Zr0.5Hf0.5Ni0.8Pd0.2Sn0.99Sb0.01 alloy with nanophase inclusión. J Appl Phys 2006;99. 064305(1–6).
[108] [108] Poon JS, Wu D, Zhu S, Xie W, Tritt TM, Thomas P, et al. Half-Heusler phases and nanocomposites as emerging high-ZT thermoelectric materials. J Mater Res 2011;26:2795–802.
[109] Makongo JPA, Misra DK, Zhou X, Pant A, Shabetai MR, Su X, et al. Simultaneous large enhancements in thermopower and electrical conductivity of bulk nanostructured half-Heusler alloys. J Am Chem Soc 2011;133:18843–52.
[110] Sahoo P, Liu Y, Makongo Julien PA, Su XL, Kim SJ, Takas N, et al. Enhancing thermopower and hole mobility in bulk p-type half-Heuslers using fullHeusler nanostructures. Nanoscale 2013;5:9419–27.

[111] Sakurada S, Shutoh N, Hirono S. Thermoelectric material and thermoelectric device. US patent 7745720 B2, 2010 June 29.
[112] Shuai J, Mao J, Song S, Zhang Q, Chen G, Ren Z. Recent progress and future challenges on thermoelectric Zintl materials. Mater Today Phys. 2017;1:74-95.
[113] Cooley JA, Promkhan P, Gangopadhyay S, et al. High Seebeck coefficient and unusually low thermal conductivity near ambient temperatures in layered compound $Yb_{2-x}Eu_xCdSb_2$. Chem Mater. 2017;30:484-493.
[114] Hu Y, Wang J, Kawamura A, Kovnir K, Kauzlarich SM. Yb14MgSb11 and Ca14MgSb11-new mg-containing Zintl compounds and their structures, bonding, and thermoelectric properties. Chem Mater. 2014;27:343-351.
[115] Bhardwaj A, Misra D. Enhancing thermoelectric properties of a p-type Mg3Sb2-based Zintl phase compound by Pb substitution in the anionic framework. RSC Adv. 2014;4:34552-34560.
[116] Kauzlarich SM, Brown SR, Snyder GJ. Zintl phases for thermoelectric devices. Dalton Trans. 2007;2007:2099-2107.
[117] Y. Pei, X. Shi, A. LaLonde, H. Wang, L. Chen, G.J. Snyder, Nature 473 (2011) 66–69.
[118] H. Wang, Y. Pei, A.D. LaLonde, G.J. Snyder, Proc. Natl. Acad. Sci. U. S. A. 109 (2012) 9705–9709.
[119] E.S. Toberer, A. Zevalkink, G.J. Snyder, J. Mater. Chem. 21 (2011) 15843.
[120] H. Tamaki, H.K. Sato, T. Kanno, Adv. Mater. 28 (2016) 10182–10187.
[121] W. Peng, G. Petretto, G.-M. Rignanese, G. Hautier, A. Zevalkink, Joule 2 (2018) 021303.
[122] A. Zevalkink, J. Swallow, G.J. Snyder, Dalton Trans. 42 (2013) 9713–9719.
[123] G.S. Pomrehn, A. Zevalkink, W.G. Zeier, A. van de Walle, G.J. Snyder, Angew. Chem. Int. Ed. Engl. 53 (2014) 3422–3426.
[124] H. Zhang, M. Baitinger, M.B. Tang, Z.Y. Man, H.H. Chen, X.X. Yang, Y. Liu, L. Chen, Y. Grin, J.T. Zhao, Dalton Trans. 39 (2010) 1101–1104.
[125] J.J. Kuo, S.D. Kang, K. Imasato, H. Tamaki, S. Ohno, T. Kannoc, G.J. Snyder, Energy Environ. Sci. 11 (2018) 429–434.
[126] A. Zevalkink, E.S. Toberer, W.G. Zeier, E. Flage- Larsen, G.J. Snyder, Energy Environ. Sci. 4 (2011) 510–518.
[127] A. Zevalkink, W.G. Zeier, G. Pomrehn, E. Schechtel, W. Tremel, G.J. Snyder, Energy Environ. Sci. 5 (2012) 9121.
[128] B.R. Ortiz, P. Gorai, L. Krishna, R. Mow, A. Lopez, R. McKinney, V. Stevanović, E.S. Toberer, J. Mater. Chem. A 5 (2017) 4036–4046.
[129] J. Yan, P. Gorai, B. Ortiz, S. Miller, S. Barnett, T. Mason, V. Stevanovic, E.S. Toberer, Energy Environ. Sci. 8 (2015) 983–994.
[130] L. jerg, G.K.H. Madsen, B.B. Iversen, Chem. Mater. 24 (2012) 2111–2116.
[131] B.R. Ortiz, P. Gorai, V. Stevanović, E.S. Toberer, Chem. Mater. 29 (2017) 4523–4534.
[132] J. Zhang, L. Song, S.H. Pedersen, H. Yin, L.T. Hung, B.B. Iversen, Nat. Comm. 8 (2016) 13901.